ISSN: 2582-7219



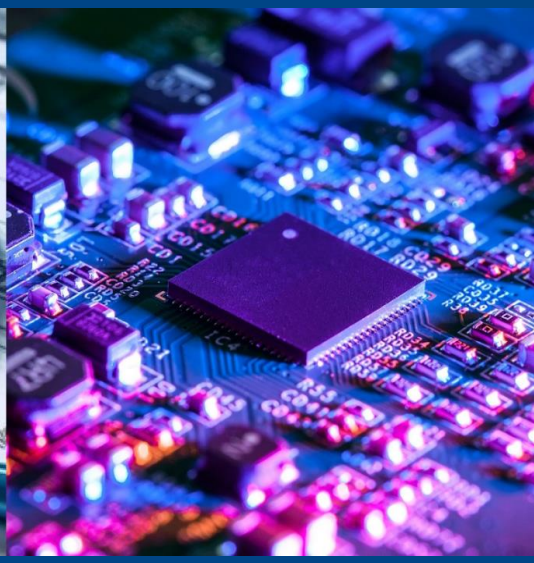

International Journal of Multidisciplinary Research in Science, Engineering and Technology

(A Monthly, Peer Reviewed, Refereed, Scholarly Indexed, Open Access Journal)


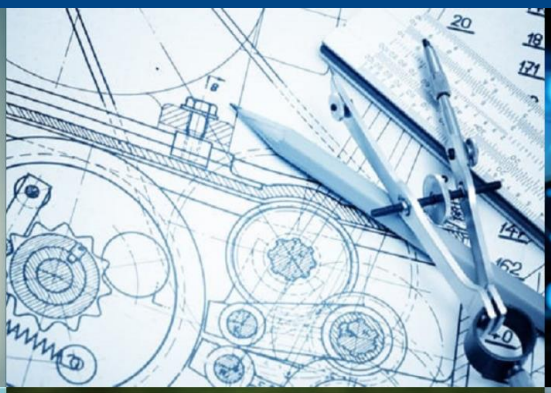

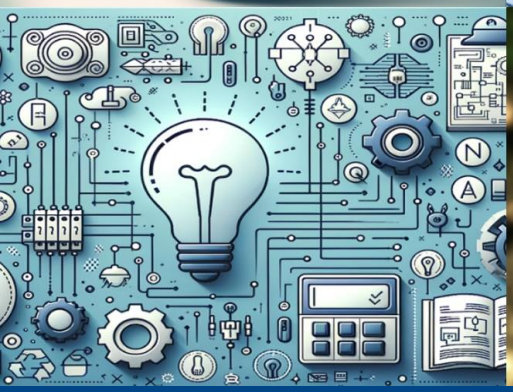

Impact Factor: 8.206 **Volume 9, Issue 3, March 2026**

© 2026 IJMRSET | Volume 9, Issue 3, March 2026| DOI:10.15680/IJMRSET.2026.0903004

ISSN: 2582-7219 | www.ijmrset.com | Impact Factor: 8.206| ESTD Year: 2018|

International Journal of Multidisciplinary Research in Science, Engineering and Technology (IJMRSET)

(A Monthly, Peer Reviewed, Refereed, Scholarly Indexed, Open Access Journal)

Litho-Fabric deformation in the meta-sedimentary rocks of Ogotun, Ikeji, and Ipetu, Southwestern Nigeria: Implications on mineralization control

Olususi Joseph Ige[1], Ayodele Olusiji Samuel[2], and Adebisi Matthew Iwabi[3]

Nigerian Geological Survey Agency, Southwest Zonal Office, Ibadan, Oyo State, Nigeria. [1]

Email: tjossey94@gmail.com

Department of Applied Geology, the Federal University of Technology, Akure, Ondo State, Nigeria. [2]

Email: osayodele@futa.edu.ng

Department of Applied Geology, the Federal University of Technology, Akure, Ondo State, Nigeria. [3]

Email: adebisi.iwabi@gmail.com

Corresponding author*: Email: adebisi.iwabi@gmail.com
Phone Number: +234 806 040 4995
ORCID ID: 0009-0006-6363-4854

ABSTRACT: This study investigates the litho-structural characteristics of meta-sedimentary rocks in Ogotun, Ikeji, and Ipetu, southwestern Nigeria, to evaluate geological controls on mineralization within the Pan-African basement complex. Remote sensing, aeromagnetic data, field mapping, and petrography were integrated to delineate structural features, characterize lithologies, and assess their influence on mineralization. Sentinel-2A imagery was enhanced using Principal Component Analysis for lineament extraction, while aeromagnetic data were analyzed with Total Magnetic Intensity, Reduction to the Equator, analytic signal, derivative filters, and Euler Deconvolution to reveal subsurface structures and estimate source depths. Field mapping and petrography characterized lithology, mineralogy, and deformation fabrics. NE–SW and E–W lineaments dominate the structural framework, reflecting polyphase Pan-African deformation. Surface fracture density is relatively low in migmatite and granite, whereas aeromagnetic data reveal short, discontinuous fractures. Euler Deconvolution indicates source depths of ~1000–2500 m. Petrography shows quartz, biotite, muscovite, plagioclase, microcline, and chalcopyrite inclusions in quartz schist. Lithological heterogeneity and hydrothermal alteration appear to control mineralization more than surface fractures, with deeper lithologically favorable zones being the most prospective

KEYWORDS: Ogotun, Epigenetic mineralization, Meta-conglomerate, Hydrothermal mineralization, Pan-African.

I. INTRODUCTION

Lithological and structural mapping is critical for understanding the geological framework and mineralization potential, especially in areas with limited data. In complex basement terrains, integrating remote sensing, aeromagnetic surveys, and field observations effectively delineates lithological units and structural features controlling mineralization (Prasad et al., 2023; Hu, 2025). Aeromagnetic data capture variations in subsurface magnetic properties, while satellite imagery highlights surface lithological and structural variations, providing complementary information for improved interpretation (Agrawal et al., 2023; Senanayake et al., 2023). Mineral deposits in Precambrian basement terrains are often controlled by lithological contacts, faults, fractures, and shear zones that channel hydrothermal fluids (Wu et al., 2025; Wang, 2025). In southwestern Nigeria, significant mineralization occurs in the Precambrian Basement Complex, particularly within the Ilesha Schist Belt. The study areas—Ogotun, Ikeji-Ile, and Ipetu—represent poorly documented portions of this belt. This study integrates remote sensing, aeromagnetic interpretation, field mapping, and petrography to characterize litho-structural deformation and assess its influence on mineralization.

© 2026 IJMRSET | Volume 9, Issue 3, March 2026| DOI:10.15680/IJMRSET.2026.0903004

ISSN: 2582-7219 | www.ijmrset.com | Impact Factor: 8.206| ESTD Year: 2018|

International Journal of Multidisciplinary Research in Science, Engineering and Technology (IJMRSET)

(A Monthly, Peer Reviewed, Refereed, Scholarly Indexed, Open Access Journal)

II. DESCRIPTION OF THE STUDY AREA

The study area is located in southwestern Nigeria (latitudes 7°27′–7°32′N, longitudes 4°52′–5°02′E), covering ~170 km² across parts of Ekiti and Osun States,**Fig. 1,** including Ogotun, Ikeji-Ile, and Ipetu-Ijesha within the Ilesha Schist Belt. This Pan-African basement terrain is characterized by polyphase tectonism, regional metamorphism, and extensive granitoid intrusions, producing complex lithological and structural heterogeneity. The terrain is rugged, with low- to moderate-relief hills, inselbergs, and exposed bedrock along valleys and streams, underlain by metamorphic and meta-sedimentary rocks. Dendritic drainage reflects the control of basement lithology and structural fabrics. Foliations, folds, fractures, and shear zones are widespread, forming potential pathways for hydrothermal fluids and influencing mineralization, making the area suitable for studying litho-structural deformation and its impact on metallic mineralization (Rahaman, 1988). .

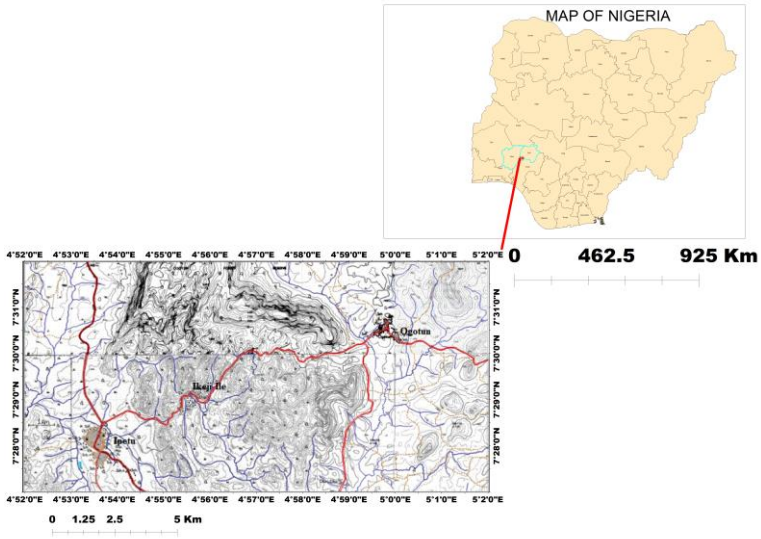

Figure 1: Map of the study area located within Ekiti and Osun States, southwestern Nigeria**,** showing the spatial extent of the investigated region. The map highlights the major towns and geographical boundaries within the study area. Inset**:** Map of Nigeria indicating the regional location of the study area within the southwestern part of the country.

III. MATERIALS AND METHODS

3.1 Data acquisition

Sentinel-2A multispectral imagery (10–60 m resolution) from the Copernicus Open Access Hub was used for lithological and structural mapping. Aeromagnetic data from the Nigerian Geological Survey Agency were acquired along NW–SE lines (500 m spacing) with NE–SW tie lines (5000 m), corrected for diurnal variation, drift, and the geomagnetic field (Agrawal et al., 2023; Senanayake et al., 2023).

3.2 Remote sensing and mineral mapping

Sentinel-2A imagery was enhanced via Principal Component Analysis in ENVI 5.0, and lineaments were extracted in ArcGIS 10.5. Lineament density and rose diagrams were produced in RockWorks 17 to summarize structural trends. Band ratio techniques highlighted lithological variations and potential alteration zones (Wu et al., 2025; Wang, 2025).

3.3 Aeromagnetic data processing

Aeromagnetic grids were processed in Oasis Montaj. Total Magnetic Intensity, Reduction to the Equator, First Vertical Derivative, and Analytic Signal maps were generated to delineate lithological contacts and structures. Euler Deconvolution (SI = 0.5 and 1) estimated depths and locations of magnetic sources, revealing faults, fractures, and structural trends (Wu et al., 2025; Wang, 2025).

ISSN: 2582-7219 | www.ijmrset.com | Impact Factor: 8.206| ESTD Year: 2018|

International Journal of Multidisciplinary Research in Science, Engineering and Technology (IJMRSET)

(A Monthly, Peer Reviewed, Refereed, Scholarly Indexed, Open Access Journal)

3.4 Field and laboratory work

Field mapping (1:25,000) recorded lithology, foliation, joints, and fractures using GPS and a Brunton compass. Thirty-two rock samples were collected, with fifteen selected for petrographic analysis. Thin sections were examined under transmitted light microscopy, and polished sections were analyzed under reflected light for ore mineral identification.

IV. RESULTS AND DISCUSSIONS

4.1 Remote sensing

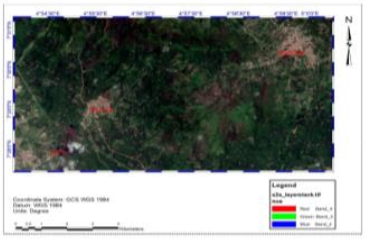

Figure 2: Sentinel-2A multispectral imagery of the study area showing the surface geological features and structural patterns used for lineament extraction and lithological interpretation.

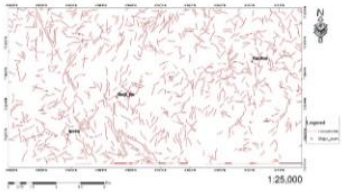

Figure 3: Sentinel-2A–derived lineament map of the study area showing the spatial distribution and orientation of structural features interpreted from the processed imagery.

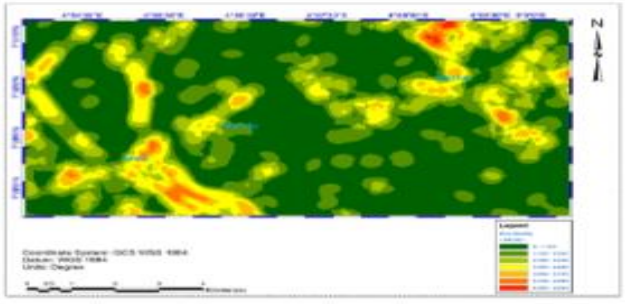

Figure 4: Lineament density map of the study area derived from Sentinel-2A

Figure 2 presents the Sentinel-2A false-color composite (RGB = 4-3-2) of Ogotun, Ikeji-Ile, and Ipetu-Ijesha, highlighting variations in vegetation, land cover, and exposed bedrock. Dense vegetation appears dark green, while sparsely vegetated and cultivated areas are lighter green or brown, often coinciding with rock outcrops suitable for geological mapping and sampling. Linear and curvilinear features trending NW–SE and NE–SW are evident, representing fractures and faults within the Ilesha Schist Belt, providing preliminary structural control information (Wu et al., 2025; Wang, 2025).

Figure 3 shows the Sentinel-2A–derived lineament map, with red lines indicating faults, fractures, and foliation trends. Predominant NW–SE and NE–SW orientations reflect the regional tectonic fabric (Rahaman, 1988). Zones of higher lineament density may indicate enhanced permeability and potential mineralization, whereas sparse areas correspond to more competent basement rocks. **Figure 4** depicts the lineament density map, illustrating spatial variations across the study area. High-density zones, notably in banded gneiss and quartzite, reflect pervasive deformation and weathering NW–SE and NE–SW trends align with regional tectonic fabrics, and integrating these maps with field and aeromagnetic data supports lithological delineation and targeted mineral exploration (Wu et al., 2025; Wang, 2025).

ISSN: 2582-7219 | www.ijmrset.com | Impact Factor: 8.206| ESTD Year: 2018|

International Journal of Multidisciplinary Research in Science, Engineering and Technology (IJMRSET)

(A Monthly, Peer Reviewed, Refereed, Scholarly Indexed, Open Access Journal)

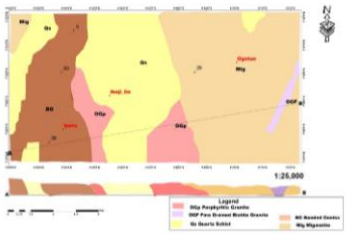

Figure 5: Geological map and representative cross-sections of the study area showing the distribution of major lithological units and structural relationships.

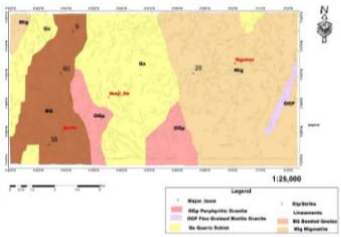

Figure 6: Lineaments superimposed on the geological map, showing the spatial distribution and orientation of major and minor structural features within the study area.

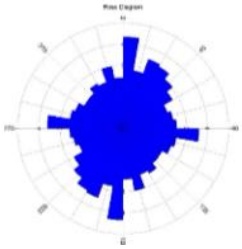

Figure 7: Rose diagram of the study area, showing the orientation and frequency of lineaments.

Figure 5 shows the geological map and A–B cross-section of the study area, highlighting five major units: Migmatite (Mig), Banded Gneiss (BG), Quartz Schist (Qs), Porphyritic Granite (OGp), and Fine-Grained Biotite Granite (OGF). The lithologies exhibit a NNE–SSW structural grain, with Quartz Schist forming metasedimentary troughs and Older Granites intruded along pre-existing structures (Rahaman, 1988). Cross-section dips (~28°–60°) indicate crustal shortening during Pan-African orogenesis. Euler Deconvolution shows shallow sources in fractured schists (<1500 m) and deeper granitic roots (>2000 m), emphasizing structurally complex zones favorable for hydrothermal fluid flow and groundwater.

Figure 6 presents lineaments superimposed on geology, revealing a multidirectional brittle deformation network. Higher lineament density occurs in Quartz Schist and Banded Gneiss, while granites are massive and less fractured (Prasad et al., 2023; Hu, 2025). Dominant trends are NNE–SSW and NE–SW, with cross-cutting structures indicating post-granite deformation. These lineament patterns highlight zones of enhanced permeability and potential mineralization. **Figure 7** shows a rose diagram summarizing structural trends, with primary NNE–SSW to NE–SW orientations (~10°–40°) and secondary E–W to ENE–WSW trends (~80°–100°), consistent with regional Pan-African fabrics (Rahaman, 1988). Minor WNW–ESE and NW–SE peaks suggest local stress perturbations or pluton-related reactivation, identifying fracture intersections likely to control hydrothermal mineralization and groundwater flow (Wu et al., 2025; Wang, 2025).

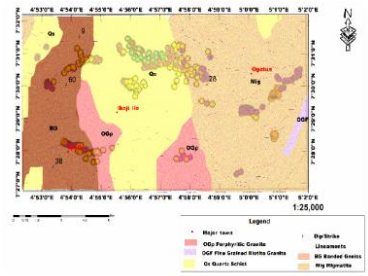

Figure 8: Euler deconvolution results overlaid on the geological map of the study area, showing the interpreted lineaments and depth estimates of subsurface structures.

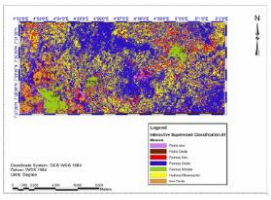

Figure 9: Mineralogical map of the study area, illustrating the spatial distribution of key rock-forming and ore-related minerals.

ISSN: 2582-7219 | www.ijmrset.com | Impact Factor: 8.206| ESTD Year: 2018|

International Journal of Multidisciplinary Research in Science, Engineering and Technology (IJMRSET)

(A Monthly, Peer Reviewed, Refereed, Scholarly Indexed, Open Access Journal)

Figure 8 shows Euler Deconvolution solutions overlaid on the geological map and lineaments, revealing the depth and location of magnetic sources relative to lithology and structures. Clusters occur along contacts between Quartz Schist (Qs), Banded Gneiss (BG), Migmatite (Mig), and Porphyritic Granite (OGp), particularly near Ipetu, indicating shallow to intermediate sources controlled by fractures and faults. In central and eastern sectors, solutions align with NE–SW and NNE–SSW lineaments and granitic contacts, reflecting deeper, structurally controlled intrusions. Integration with lithological and structural data highlights a heterogeneous, deformed basement with fracture zones favorable for hydrothermal fluids and mineralization.

Figure 9 presents the mineralogical map from supervised classification of multispectral imagery. Iron oxides, ferrous silicates, and hydroxyl-bearing minerals are unevenly distributed, reflecting lithology, alteration, and weathering. Ferrous silicates dominate migmatites and banded gneisses, ferric oxides concentrate in quartz schist and granites, and hydroxyl-bearing minerals occur along structurally controlled zones. Alignment of mineral clusters with NNE–SSW structures indicates tectonic control on surface mineralogy and supports identification of prospective mineralized zones (Rahaman, 1988).

4.2 Aeromagnetic Data

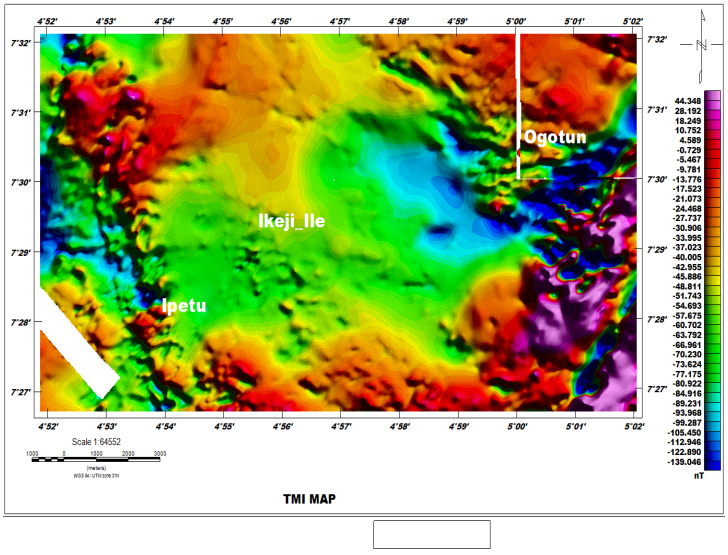

Figure 10: Total Magnetic Intensity (TMI) map of the study area, showing the spatial

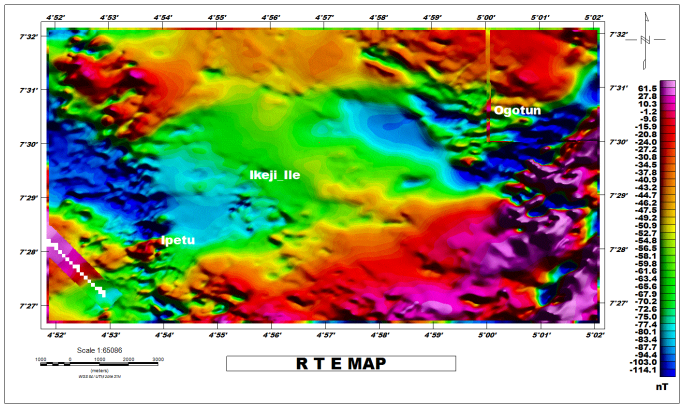

Figure 11: Reduced-to-Equator (RTE) magnetic map of the study area, showing the corrected magnetic anomalies with respect to the equator.

© 2026 IJMRSET | Volume 9, Issue 3, March 2026| DOI:10.15680/IJMRSET.2026.0903004

ISSN: 2582-7219 | www.ijmrset.com | Impact Factor: 8.206| ESTD Year: 2018|

International Journal of Multidisciplinary Research in Science, Engineering and Technology (IJMRSET)

(A Monthly, Peer Reviewed, Refereed, Scholarly Indexed, Open Access Journal)

Figure 10 shows the Total Magnetic Intensity (TMI) map, highlighting variations in magnetic susceptibility. High-amplitude anomalies (pink–red) occur mainly in Migmatite–Gneiss and Older Granite areas, reflecting magnetite- and biotite-rich rocks, while low-amplitude zones (blue–green) correspond to quartz schist and banded gneiss. The map reveals a dominant NNE–SSW to NE–SW structural fabric, with sharp gradients marking lithological contacts, faults, or shear zones that align with surface lineaments **Fig. 7**. Strong gradients indicate potential hydrothermal pathways, while broad magnetic lows suggest deeper basement or thick weathered cover suitable for groundwater (Wu et al., 2025; Wang, 2025). **Figure 11** presents the Reduced-to-Equator (RTE) map, correcting for low-latitude inclination and positioning anomalies above their sources. Low anomalies (blue–green) near Ikeji-Ile correspond to felsic lithologies, deep weathering, or hydrothermal alteration, whereas high anomalies (yellow–red–purple) in the northeast and south indicate magnetite-rich or shallow basement rocks. NE–SW, NW–SE, and local E–W linear features represent faults, fractures, shear zones, or lithological contacts, reflecting Pan-African structural control and potential hydrothermal fluid pathways (Agrawal et al., 2023; Senanayake et al., 2023).

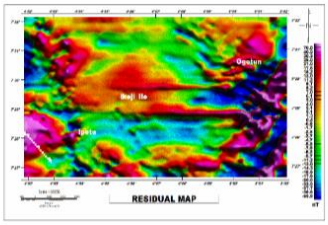

Figure 12: Residual anomaly map of the study area, highlighting localized magnetic variations after the regional field has been removed.

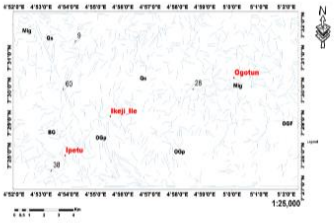

Figure 13: Lineament map of the study area, showing the orientation, distribution, and density of structural features derived from satellite imagery and geological data.

Figure 12 shows the Residual Magnetic Anomaly (RMA) map, isolating short-wavelength anomalies from the Total Magnetic Intensity (TMI) to highlight shallow sources (Agrawal et al., 2023; Senanayake et al., 2023). Magnetic values range from −65.5 nT to 70.8 nT, reflecting heterogeneous basement susceptibility. Moderate to high positive anomalies (red–orange) near Ikeji-Ile indicate shallow magnetite-bearing rocks such as amphibolites, charnockites, or mafic intrusives, while low anomalies (blue–cyan) in Ipetu and Ogotun correspond to felsic lithologies, deep weathering, or hydrothermal alteration (Ige et al., 2026). Linear NE–SW and NW–SE anomalies represent faults, fractures, shear zones, or lithological contacts, with NE–SW trends reflecting Pan-African tectonic fabric and potential hydrothermal pathways (Wu et al., 2025; Wang, 2025).

Figure 13 presents the lineament map, showing structural features derived from geophysical and remote sensing data. Lineaments indicate faults, fractures, shear zones, and lithological contacts that control deformation and may channel hydrothermal fluids. A dense network occurs around Ikeji-Ile, Ipetu, and Ogotun, predominantly NE–SW and NW–SE with minor E–W trends, consistent with the Pan-African structural grain (~600 Ma) (Rahaman, 1988). Intersecting lineaments suggest zones of enhanced fracture connectivity, favorable for mineral deposition and groundwater accumulation (Agrawal et al., 2023; Senanayake et al., 2023).

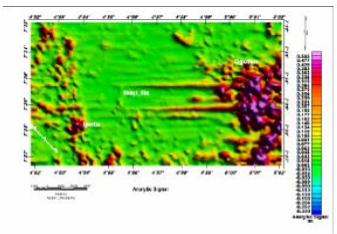

Figure 14: Analytical signal map of the study area, highlighting the edges of magnetic sources and delineating subsurface structures.

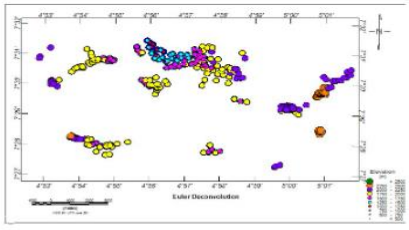

Figure 15: Euler Deconvolution map of the study area, showing estimated depths and locations of magnetic sources.

ISSN: 2582-7219 | www.ijmrset.com | Impact Factor: 8.206| ESTD Year: 2018|

International Journal of Multidisciplinary Research in Science, Engineering and Technology (IJMRSET)

(A Monthly, Peer Reviewed, Refereed, Scholarly Indexed, Open Access Journal)

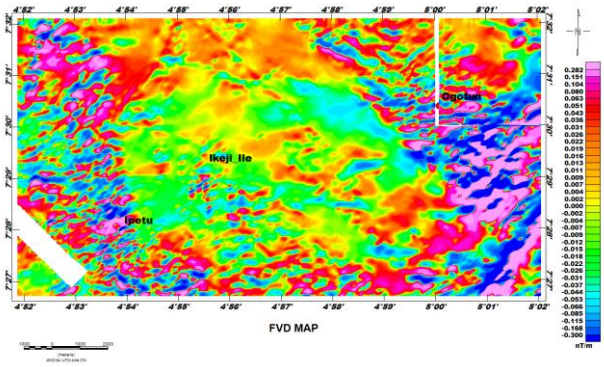

Figure 14 shows the Analytic Signal (AS) map, which highlights edges of magnetized bodies independent of magnetization direction, ideal for low-latitude regions (Agrawal et al., 2023; Senanayake et al., 2023). High-amplitude anomalies (magenta–purple) occur near Ogotun and Ipetu, corresponding to strong magnetic contrasts at lithological contacts between Older Granites (OGp) and Migmatite-Gneiss. Circular or lobate anomalies suggest shallow intrusions, while linear ridges trending E–W and NE–SW mark faults, shear zones, or lithological boundaries. Figure 15 presents Euler Deconvolution (ED) solutions, estimating depths of magnetic sources (SI = 1). Shallow sources (~1250–1750 m) near Ikeji-Ile and Ipetu coincide with high lineament density, indicating fractured basement favorable for fluid migration and mineralization. Deeper sources (~2000–2500 m) in the east align with Older Granite intrusions. Clustering along NNE–SSW trends validates major fault systems, while convergence of solutions indicates interconnected fracture networks controlling groundwater and hydrothermal pathways (Agrawal et al., 2023; Senanayake et al., 2023). Figure 16 emphasizes shallow magnetic sources and high-frequency structures often obscured in TMI maps. Rapid color transitions (reds/pinks to blues/greens) mark numerous shallow bodies, with positive anomalies reflecting magnetic lithologies (mafic dykes, mineralized zones, basement highs) and negative anomalies representing less magnetic rocks, alteration zones, or sedimentary cover. NE–SW and NW–SE linear features reflect intersecting faults and fractures controlling lithological contacts (Prasad et al., 2023; Hu, 2025).

Table 1. Field data of rock samples collected from the study area, showing sample ID, location coordinates, lithology, observed structures, and key field remarks (Ige et al., 2026).

ID	Location	Lat (°N)	Lon (°E)	Rock Type	Structures	Remarks
1	Ori-oke, Ogotun	07°30.05	04°58.751	Migmatite Gneiss	Exfoliation, weathering	–
2	Okemi (Pa Tunji), Ogotun	07°30.453	05°00.062	Migmatite Gneiss	Fractures, dykes, veins	–
3	Off Igbara Odo Rd, Ogotun	07°30.571	05°00.127	Migmatite Gneiss	Solution holes, exfoliation	–
4	Okemi (1), Ogotun	07°30.598	05°00.760	Migmatite Gneiss	Xenoliths, boulders, pegmatite	–
5	Okemi (2), Ogotun	07°29.569	05°01.039	Migmatite Gneiss	Dykes, folds, solution holes	–
6	Otapete, Ogotun	07°28.863	05°00.876	Migmatite Gneiss	Solution holes, pegmatite	–
7	St Jude's ANG, Ikeji-Ile	07°28.970	04°55.565	Quartz Schist	Joints, quartz vein	Strike 300°SE, Dip 80°W
8	Beside Sericoco Hotel, Ipetu	07°27.213	04°54.051	Porphyritic Granite	Fractures, joints	–
9	Kristal V. Ltd Quarry, Ipetu	07°29.569	04°53.891	Porphyritic Granite	Pegmatite intrusion	–
10	Araromi, Ipetu	07°28.495	04°53.577	Metaconglomerate	Crenulations, xenolith	–
11	Under power line,	07°28.913	04°54.454	Migmatite Gneiss	Xenoliths, solution holes	–

© 2026 IJMRSET | Volume 9, Issue 3, March 2026| DOI:10.15680/IJMRSET.2026.0903004

ISSN: 2582-7219 | www.ijmrset.com | Impact Factor: 8.206| ESTD Year: 2018|

International Journal of Multidisciplinary Research in Science, Engineering and Technology (IJMRSET)

(A Monthly, Peer Reviewed, Refereed, Scholarly Indexed, Open Access Journal)

ID	Location	Lat (°N)	Lon (°E)	Rock Type	Structures	Remarks
	Ikeji-Ile Rd					
12	Oke Ayile, Ikeji-Ile	07°30.047	04°55.780	Porphyritic Granite	Xenoliths, joints	–
13	Oke Arifo, Ikeji-Ile	07°30.223	04°55.689	Porphyritic Granite	Pegmatitic intrusion, xenolith	–
14	Off Ikeji-Ile Rd, Ipetu	07°29.317	04°56.006	Quartzite	Schistosity	Strike 42°SW
15	Off Ilesha Rd, Ipetu	07°30.037	04°53.827	Quartz Schist	Fine-medium grain, muscovite & biotite	Strike 180°NE, Dip 58°W

Table 1 summarizes field observations from fifteen locations in the Ijesha/Ipetu-Ijesha region. Migmatite gneiss (samples 1–6, 11) dominates, showing exfoliation, pegmatite intrusions, and xenoliths, reflecting Pan-African deformation and partial melting (Rahaman, 1988). Quartz schist (samples 7, 15) exhibits foliation, jointing, and aligned micas, controlling fractures and fluid flow. Porphyritic granites (samples 8, 9, 12, 13) show pegmatites and joints, indicating post-tectonic emplacement. Metaconglomerate (sample 10) and quartzite (sample 14) display metamorphic fabrics and alignment of quartz grains. These features confirm mapped lithologies and lineaments, emphasizing a structurally complex basement influencing fluid migration, mineralization, and groundwater (Prasad et al., 2023; Hu, 2025).

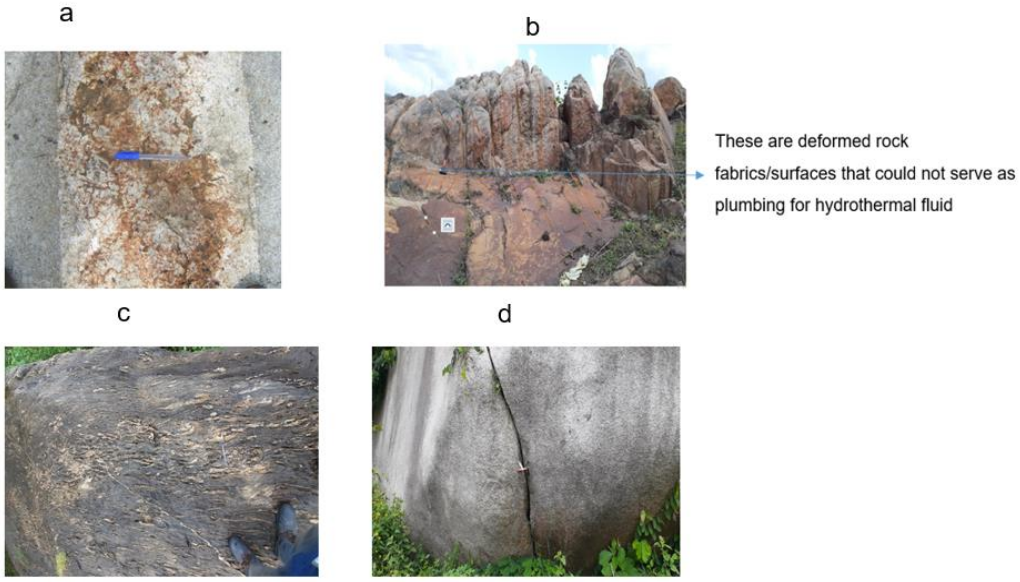

Figure 17: Field photographs of representative lithologies and structural features within the study area: (a) migmatite–gneiss outcrop intruded by pegmatite at Otapete, Ogotun (Long. 05°00.876′E, Lat. 07°28.970′N); (b) quartz schist exposure at Ikeji-Ile showing well-developed foliation (Long. 04°55.565′E, Lat. 07°28.970′N); (c) metaconglomerate outcrop at Araromi–Ipetu (Long. 04°53.577′E, Lat. 07°28.495′N); and (d) porphyritic granite displaying prominent deep fractures at Ipetu (Long. 04°54.051′E, Lat. 07°27.213′N).

Figure 17: Field photographs showing lithological diversity and structural features: (a) migmatite–gneiss at Ogotun with pegmatite intrusions, reflecting Pan-African deformation and partial melting (Rahaman, 1988); (b) quartz schist at Ikeji-Ile with steep foliation aligned with NNE–SSW trends; (c) deformed metaconglomerate at Araromi–Ipetu; (d) porphyritic granite at Ipetu with deep fractures enhancing fluid pathways (Prasad et al., 2023; Hu, 2025). These observations indicate interconnected ductile and brittle structures controlling mineralization potential.

© 2026 IJMRSET | Volume 9, Issue 3, March 2026| DOI:10.15680/IJMRSET.2026.0903004

ISSN: 2582-7219 | www.ijmrset.com | Impact Factor: 8.206| ESTD Year: 2018|

International Journal of Multidisciplinary Research in Science, Engineering and Technology (IJMRSET)

(A Monthly, Peer Reviewed, Refereed, Scholarly Indexed, Open Access Journal)

Table 2. Modal Mineralogy of 15 Rock Samples from the Study Area**.** This table summarizes the quantitative mineral composition of the collected rocks, showing proportions of Quartz (Qtz), Plagioclase (Plag), Microcline (Micro), Orthoclase (Ortho), Biotite (Biot), Hornblende (Horn), and Opaque (Opa).

S/N	Lithology	Sample / Location	Qtz	Plag	Micro	Ortho	Biot	Horn	Opa	Total
1	Migmatite Gneiss	Ikeji-Ile Rd, Ogotun	72.0	8.68	7.89	-	9.8	-	2.94	100
2	Migmatite Gneiss	PA Tunji Comp., Ogotun	81.48	2.78	1.85	-	13.89	-	-	100
3	Migmatite Gneiss	Okemi (1), Ogotun	71.34	6.95	3.47	-	14.79	-	3.48	100
4	Migmatite Gneiss	Okemi (2), Ogotun	47.62	41.9	-	-	6.66	9.2	3.8	100
5	Migmatite Gneiss	Off Igbara-Odo Rd	42.1	-	25	-	17.1	9.2	6.58	100
6	Migmatite Gneiss	Otapete Farm	45.6	-	52	-	-	-	2.4	100
7	Migmatite Gneiss	Under power line	72.72	5.68	5.68	4.58	5.68	-	5.68	100
8	Schistose Quartzite	Off Ikeji-Ile Rd, Ipetu	67.02	10.10	15	-	15.42	-	2.12	100
9	Quartz Schist	St Jude's ANG, Ikeji-Ile	51.0	-	-	-	38.77	-	10.23	100
10	Quartz Schist	Off Ilesha Rd, Ipetu	62.42	-	-	-	36.24	1.34	-	100
11	Metaconglomerate	Araromi, Ipetu	61.29	4.48	6.45	-	23.12	-	4.4	100
12	Porphyritic Granite	Beside Sericoco Hotel	60.94	22.58	5.66	-	10.82	-	-	100
13	Porphyritic Granite	Kristal V. Ltd Quarry	97.01	-	-	-	-	-	2.98	100
14	Porphyritic Granite	Oke Ayila, Ikeji-Ile	54.83	19.35	-	0.64	21.29	-	3.87	100
15	Porphyritic Granite	Oke Arifo, Ikeji-Ile	54.17	5.55	10.05	2.77	10.05	-	-	100

Table 2: Modal mineralogy of 15 representative rock samples showing lithological and metamorphic diversity in the Pan-African Basement Complex. Migmatite gneiss (S/N 1–7) is quartz-rich with plagioclase, microcline, and biotite, reflecting high-grade metamorphism and partial melting. Quartz schist and schistose quartzite (S/N 8–10) show strong foliation with quartz and biotite alignment. Metaconglomerate (S/N 11) retains metamorphosed sedimentary textures, while porphyritic granites (S/N 12–15) are quartz-dominant with feldspar and biotite, indicating magmatic emplacement post-dating the migmatite–gneiss. The variations reflect progressive metamorphism, partial melting, and granite intrusion during Pan-African tectonism (Rahaman, 1988).

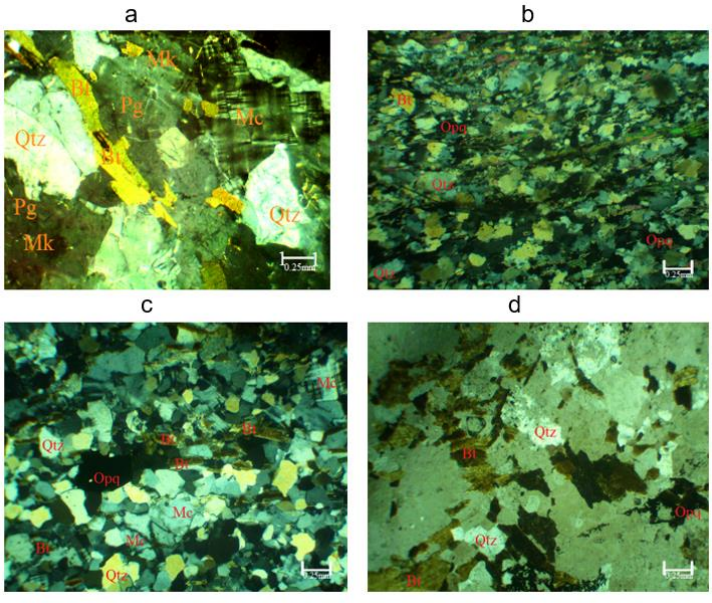

ISSN: 2582-7219 | www.ijmrset.com | Impact Factor: 8.206| ESTD Year: 2018|

International Journal of Multidisciplinary Research in Science, Engineering and Technology (IJMRSET)

(A Monthly, Peer Reviewed, Refereed, Scholarly Indexed, Open Access Journal)

Plate 1: Photomicrographs of representative lithologies from the study area under crossed nicols (Cn): (a) Migmatite–gneiss from Otapete, Ogotun (Long. 05°00.876′E, Lat. 07°28.970′N) showing microcline (Mc), quartz (Qtz), myrmekite (Mk), biotite (Bt), and plagioclase (Pg); (b) Quartz schist from Ikeji-Ile (Long. 04°55.565′E, Lat. 07°28.970′N) showing quartz (Qtz), biotite (Bt), and muscovite (Ms); (c) Metaconglomerate from Araromi–Ipetu (Long. 04°53.577′E, Lat. 07°28.495′N) showing quartz (Qtz), biotite (Bt), microcline (Mc), plagioclase (Pg), and opaques (Oq); (d) Porphyritic granite from Ipetu (Long. 04°54.051′E, Lat. 07°27.213′N) showing quartz (Qtz), biotite (Bt), orthoclase (Ort), plagioclase (Pg), and opaques (Oq).
Photomicrographs (XPL) illustrate the lithologies and metamorphic history of the Ijesha/Ipetu-Ijesha area (Plate 1).

Plate 1a: Migmatite–gneiss at Otapete, Ogotun, shows interlocking microcline, quartz, plagioclase, and myrmekite, indicating partial melting and high-grade Pan-African metamorphism. **Plate 1b**: Quartz schist at Ikeji-Ile exhibits foliation with aligned quartz, biotite, and muscovite, reflecting ductile deformation. **Plate 1c**: Metaconglomerate at Araromi–Ipetu preserves recrystallized clastic textures with quartz, biotite, microcline, plagioclase, and opaque minerals, recording metamorphosed sedimentary material. **Plate 1d**: Porphyritic granite at Ipetu contains quartz, orthoclase, and biotite phenocrysts in a fine-grained matrix, indicating two-stage cooling of plutonic magma. Together, these photomicrographs show a structurally and mineralogically diverse basement shaped by polyphase metamorphism, magmatism, and deformation, influencing fluid migration and mineralization (Rahaman, 1988; OlaOlorun).

V. CONCLUSION AND RECOMMENDATIONS

This study demonstrates that integrating Sentinel imagery with aeromagnetic data effectively maps lithology, structures, and potential mineralization in the Ogotun–Ikeji–Ipetu area of southwestern Nigeria. Remote sensing revealed multi-orientation lineaments, while aeromagnetic interpretation identified NE–SW and E–W trending magnetic lineaments reflecting polyphase Pan-African deformation. Analytic Signal and Euler Deconvolution analyses highlighted deep-seated structural discontinuities, with magnetic sources at ~1000–2500 m, suggesting hydrothermal fluid pathways and potential epigenetic mineralization. Field and petrographic data confirm five principal lithologies—migmatite–gneiss, quartzite, quartz schist, metaconglomerate, and porphyritic granites—with localized sulfide mineralization in quartz schist. Overall, lithological heterogeneity and hydrothermal alteration, rather than surface fractures, primarily control mineralization.

Recommendations: Hyperspectral remote sensing should be applied to detect alteration minerals. Detailed geological and structural mapping is encouraged to refine boundaries and identify subtle features. Future exploration should integrate geophysical, geological, petrographic, and geochemical data, with subsurface investigations (boreholes, deep sampling) targeting structurally and lithologically favorable zones.

Declarations

Ethical Approval: This study did not involve humans, animals, or clinical experiments. All data were obtained from field observations, rock sampling, and laboratory analyses, posing no ethical risk. Formal ethical approval was not required.
Consent to Participate: Not applicable, as no human participants were involved. All research adhered to standard field and laboratory protocols.
Consent to Publish: Not applicable. No personal or sensitive information is included; all data are anonymized scientific observations.
Funding: This research received no specific grant from public, commercial, or not-for-profit sectors.
Conflicts of Interest: The authors declare no competing financial or personal interests.
Availability of Data and Materials: Datasets are available from the corresponding author upon reasonable request.
Authors' Contributions: Adebisi Matthew Iwabi wrote the manuscript and interpreted results. **Ayodele Olusiji Samuel** critically reviewed and refined the manuscript. **Olususi Joseph Ige** conceptualized the study, conducted data analysis, generated maps, and contributed to structural and spatial interpretation. All authors read and approved the final manuscript.

ISSN: 2582-7219 | www.ijmrset.com | Impact Factor: 8.206| ESTD Year: 2018|

International Journal of Multidisciplinary Research in Science, Engineering and Technology (IJMRSET)

(A Monthly, Peer Reviewed, Refereed, Scholarly Indexed, Open Access Journal)

REFERENCES

(1) Ige, O. J., Samuel, A. O., Olatoye, A. M., & Iwabi, A. M. (2026).
Integrated aeromagnetic and radiometric interpretation for mineralization mapping in the Nigerian Basement Complex. International Journal of Research and Innovation in Applied Science (IJRIAS), 11(1), 531–557. https://rsisinternational.org/journals/ijrias/uploads/vol11-iss1-pg531-557-202602_pdf.pdf
(2) Agrawal, N., Govil, H., Mishra, G., Gupta, M., & Srivastava, P. K. (2023). Mapping hydrothermal alteration minerals using PRISMA hyperspectral imagery and machine learning algorithms. Remote Sensing, 15(12), 3133. https://doi.org/10.3390/rs15123133
(3) Hu, D. (2025). Research progress in the application of remote sensing technology in geological and mineral exploration. Applied and Computational Engineering, 187, 84–90.https://doi.org/10.54254/2755-2721/2025.GL27802
(4) Prasad, R., Gupta, A., & Srivastava, P. (2023). Mineral exploration employing drones, contemporary geological satellite remote sensing and GIS procedures: A review. Remote Sensing Applications: Society and Environment, 31, 100988.https://doi.org/10.1016/j.rsase.2023.100988
(5) Reddy, P. S. K., & Kottala, R. B. (2023**).** Mineral exploration methods using remote sensing and GIS techniques: A review. Journal of Remote Sensing & GIS, 14(1), 31–38.Available at: https://techjournals.stmjournals.in/index.php/JoRSG/article/view/1391
(6) Senanayake, I. P., Kiem, A. S., Hancock, G. R., Metelka, V., Folkes, C. B., Blevin, P. L., & Budd, A. R. (2023). A spatial data-driven approach for mineral prospectivity mapping using geoscience datasets. Remote Sensing, 15(16), 4074.https://doi.org/10.3390/rs15164074
(7) Wang, J. (2025**).** Research on Mineral Exploration Applications Based on Remote Sensing Technology. Applied and Computational Engineering, 186**,** 248–255.
https://direct.ewa.pub/proceedings/ace/article/view/27530
(8) Wu, E., Zhang, Y., & Li, X. (2025). Research on breakthroughs in geological and mineral exploration and the application of technology for finding minerals. Applied Mathematics and Nonlinear Sciences, 10(1).
https://doi.org/10.2478/amns-2025-0690
(9) Zamzam, S., Ghoneimi, A., Yousef, M., Hanafy, S., & Aamer, Y. (2025). Geological and iron ore mineralization mapping using remote sensing data in the Western Desert of Egypt. Bulletin of the Faculty of Science, Zagazig University.
https://doi.org/10.21608/bfszu.2024.331719.1437
(10) Rahaman, M. A. (1988).Recent Advances in the Study of the Basement Complex of Nigeria.In: Oluyide, P. O., Mbonu, W. C., Ogezi, A. E., Egbuniwe, I. G., Ajibade, A. C., & Umeji, A. C. (Eds.), Precambrian Geology of Nigeria**.** Geological Survey of Nigeria, Kaduna, pp. 11–43.https://www.sciepub.com/reference/318092

INTERNATIONAL STANDARD SERIAL NUMBER INDIA

INTERNATIONAL JOURNAL OF MULTIDISCIPLINARY RESEARCH IN SCIENCE, ENGINEERING AND TECHNOLOGY

| Mobile No: +91-6381907438 | Whatsapp: +91-6381907438 | ijmrset@gmail.com |

www.ijmrset.com